

Electrochemical deposition characteristics of p-CuSCN on n-ZnO rod arrays films

Yong Ni, Zhengguo Jin*, Ke Yu, Yanan Fu, Tongjun Liu, Tao Wang

*Key Laboratory for Advanced Ceramics and Machining Technology of Ministry of Education,
School of Materials Science and Engineering, Tianjin University, Tianjin 300072, China*

Received 8 October 2007; received in revised form 23 January 2008; accepted 29 January 2008
Available online 4 March 2008

Abstract

p-CuSCN/n-ZnO rod array heterojunctions were electrodeposited with a weak basic (pH ~9) aqueous electrolyte solution. *I*–*V* characteristics showed the heterostructure had clear rectification, indicating good electrical contacts between ZnO rod arrays and the embedded CuSCN. The energy band model for the electrodeposition of CuSCN on ZnO rod arrays was proposed based on linear sweep voltammetric (LSV) measurements, which indicated that the electrodeposition process was the prior growth of CuSCN on bare ZnO rods according to a conduction process, followed by compact filling in the gaps of the arrays based on the thermal activation mechanism of surface states. The diode properties of the heterojunctions revealed that although deposition was dominated by thermal activation mechanism of surface states, the electrodeposition should be performed at a lower temperature in order to reach fine filling of the gaps of ZnO rod arrays.

© 2008 Published by Elsevier Ltd.

Keywords: p-CuSCN; Electrochemical deposition; ZnO rod arrays; Aqueous weak basic electrolyte; Energy band model

1. Introduction

Using heterogeneous deposition on highly structured semiconductor substrates to form heterojunctions has been an attractive component in many electrical, photoelectrical, and catalytic applications where an enlargement of the interface area is generally desirable. This is especially valuable for nanocrystal photovoltaic cells (NPCs), such as dye-sensitized solar cells (DSSCs) [1] and extremely thin absorber solar cells (ETAs) [2], because of the enhancement of light trapping for photo-generated carriers and the separation efficiency of the excited carriers. The n-type electrodes of NPC solar cells have succeeded in using porous TiO₂ layers [3,4], and nanostructured columnar ZnO arrays [2,5] have also been studied for their use as the n-type electrodes supplying better electron carries transport with less grain boundaries. Generally, to effectively make use of the high internal surface of the n-type layer, the pores or gaps in the non-planar structure need to be filled completely with a p-type semiconductor layer to ensure the transport of

photo-generated carriers. As a p-type hole conducting material, CuSCN is thought to be most promising due to its transparency in the visible light spectrum range, reasonable hole conductivity ($\geq 5 \times 10^{-4} \text{ S cm}^{-1}$) [6] and chemical stability [7].

The deposition methods of CuSCN films, such as solution deposition [8], CBD [9], SILAR [9], and electrochemical deposition [1,6,10] have been reported, in which electrochemical deposition was considered to be a feasible method for coating the insides of complex shapes. Until now, studies on electrochemical deposition of CuSCN were generally performed in organic solvents because of the instability of Cu(II) cations and SCN anions in aqueous solvents [10]. Rost et al. studied electrochemical deposition of CuSCN on porous n-type TiO₂ films using purified ethanol solvent [11], and obtained a spatially distributed p–n heterojunction. However, using organic solvents led to poor conductivity of the deposition solution, dye desorption on the dye-absorbed n-type layer and poor contact with the sensitization layer [12]. Wu et al. deposited p-type CuSCN films through an EDTA-chelated copper aqueous electrolytes with pH 2–2.6 and demonstrated the advantages of the aqueous electrolytes, such as high conductivity, strong dissolvability of solutes, high deposition efficiency, and prevention of desorption of dyes [13]. More recently, Wu et al. has also investigated the electrode-

* Corresponding author.

E-mail address: zhgj@tju.edu.cn (Z. Jin).

position of CuSCN on porous TiO₂ films using such aqueous electrolytes [14]. However, the acidic aqueous electrolytes do not allow their employment on the ZnO rod array substrates due to its poor resistance to acidic etching.

Previously, we have studied the electrochemical deposition of CuSCN on ITO substrates using mild aqueous electrolytes with weakly basic pH value (~ 9) [15]. In this paper, we will focus on fine filling of CuSCN on ZnO rod arrays by the electrodeposition method to form p-CuSCN/n-ZnO rod array interpenetrating heterojunctions for the solar cell application. The morphology, junction property, and electrochemical deposition characteristics will be described.

2. Experimental

2.1. Preparation of ZnO rod electrode

ZnO rod arrays were grown on ITO glass substrates with ZnO crystalline seed layers by an aqueous chemical growth method, as explained previously [16]. First, a sol solution for ZnO seed layers was prepared by dissolving 8.2 g Zn(CH₃COO)₂·2H₂O into a mixed solution of 47.7 ml 2-methoxyethanol and 2.3 ml ethanolamine (MEA, NH₂CH₂CH₂OH) at room temperature. The cleaned ITO substrates were coated with the sol solution by a dip-coating technique and subsequently dried in an oven at 80 °C for 5 min. This dip-coating was repeated three times to increase the seed layer thickness, and the final films were annealed in air at 550 °C for 1.5 h to obtain crystalline seed layers. The aqueous growth solution for ZnO rod arrays was a mixture of 6.3 g Zn(NO₃)₂·6H₂O, 13 ml ammonia (25%) and 337 ml deionized water. The ZnO seed layer coated substrates were dipped in the growth solution at 90 °C for 4 h for the ZnO rod growth. Next, the substrates were rinsed with deionized water and air dried.

2.2. Electrodeposition of CuSCN

The electrodeposition of CuSCN films was performed on a Potentiostat/Galvanostat (TD3691, Tianjin Zhonghuan Co., China). A stable weak basic (pH ~ 9) aqueous solution, consisting of 0.01 M CuSO₄·5H₂O, 0.05 M KSCN and 0.10 M triethanolamine (TEA, N(CH₂CH₂OH)₃) [15], was used as the electrolyte. A standard three-electrode electrochemical cell con-

figuration was applied, in which the as-prepared ZnO rod arrays functioned as working electrodes, Pt foil as a counter electrode and an Ag/AgCl_{sat} as a reference electrode.

2.3. Characterization

The electrochemical measurements of CuSCN and *I*–*V* characteristics of the deposited heterostructure films were recorded on the Potentiostat/Galvanostat. Thin Au layers were vacuum-evaporated on the obtained CuSCN films for *I*–*V* measurements. The *I*–*V* measurements were performed in the sweep direction from -1.0 V to $+1.0$ V with a sweep speed of 50 mV/s. The film morphology was observed by field emission scanning electron microscope (FESEM, JEOL JSM-6700).

3. Results and discussion

To examine the chemical stability of the ZnO rod arrays in the electrolyte solution, the ZnO film was dipped into the electrolyte solution for 24 h. The surface FESEM images of the ZnO rod arrays prior to and after dipping are shown in Fig. 1. From the FESEM observation, it can be concluded that the as-prepared ZnO rods were uniform with a length of about 2 μ m and mean diameter of about 100 nm and vertically aligned to the substrate. After dipping in the electrolyte solution, the rods maintained their original morphology, suggesting that the weak basic electrolyte had little effect on the ZnO rod array morphology in spite of the long duration of dipping. This further indicates that the weak basic CuSCN electrolyte solution could be used in the following research of CuSCN electrodeposition on the ZnO rod arrays.

CuSCN was electrodeposited on ZnO rod arrays substrates at the potential of -500 mV with different deposition times and temperatures, and the FESEM images are shown in Fig. 2. Fig. 2a and b is the cross-sectional plane and the surface morphology of the sample deposited for 5 min, respectively. It can be seen that a few CuSCN grains grew on the lateral portions of ZnO rods, and there were no CuSCN grains grown on the top of ZnO rods. For the sample deposited for 15 min (Fig. 2c and d), we can clearly see the CuSCN deposit had wrapped around the ZnO rods, particularly in the area denoted by an arrow. After 1 h of deposition (Fig. 2e), the gaps among the ZnO rods had

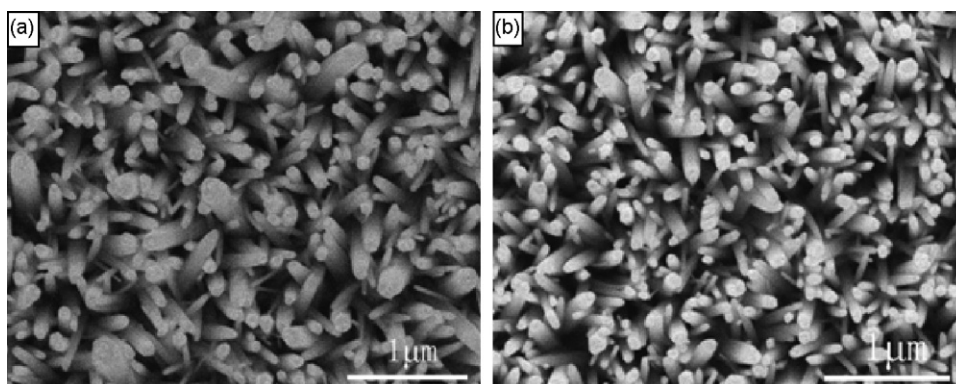


Fig. 1. FESEM images of the ZnO rod arrays: (a) as-grown and (b) following dipping in the electrolyte solution for 24 h.

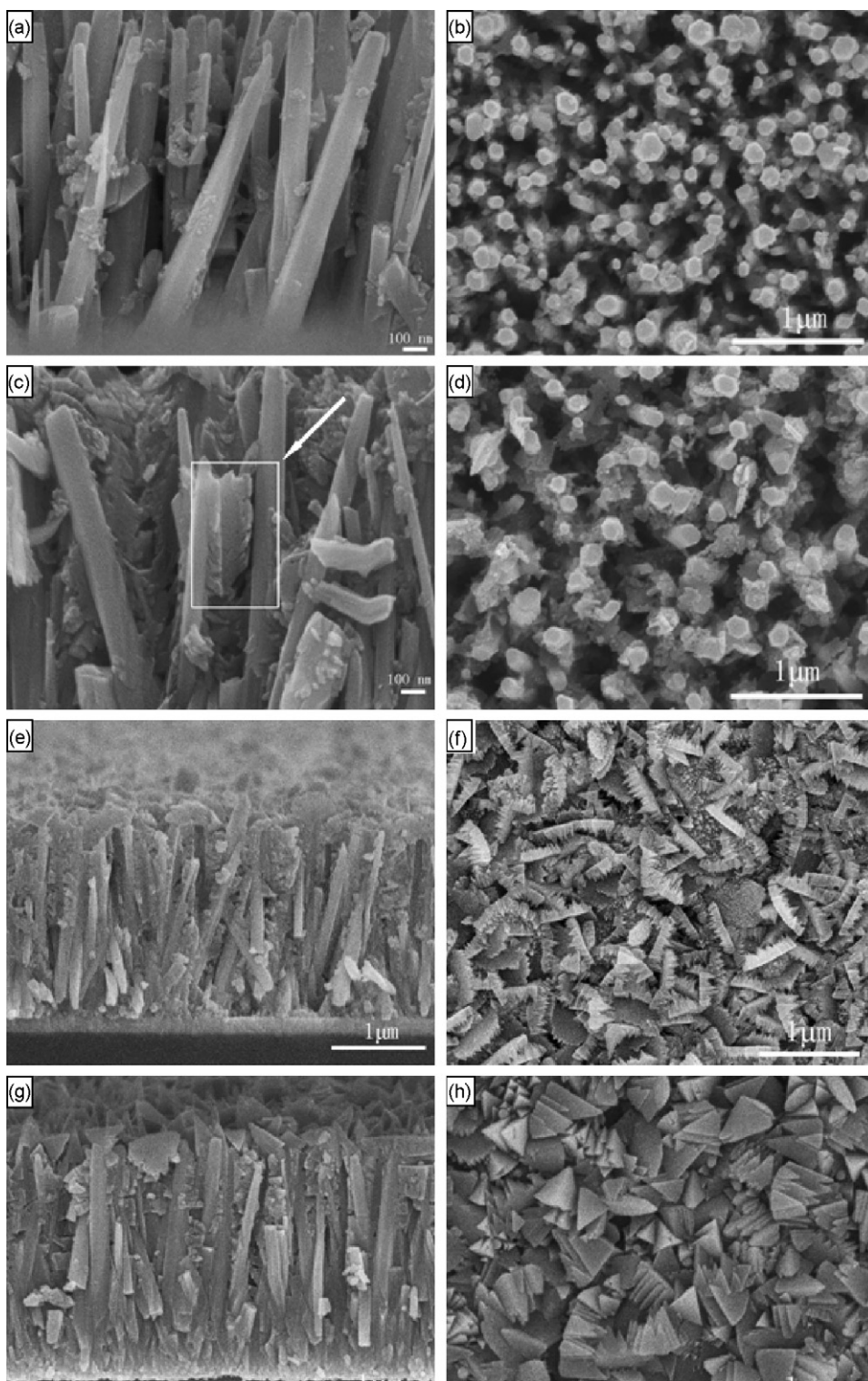


Fig. 2. FESEM images of cross-sectional and top views of electrodeposited CuSCN on ZnO rod arrays with different deposition time (a) and (b) 5 min, (c) and (d) 15 min, (e) and (f) 1 h, at the potential of -500 mV and temperature 0 °C. (g) and (h) were prepared at -500 mV and 20 °C for 1 h deposition.

been fully filled by stacked small CuSCN grains. From these FESEM images, it is clear that every single ZnO rod works as an electrode, on which the reduction of cupric ions (Cu^{2+}) to cuprous ions (Cu^+) and the deposition of CuSCN occurs locally. Moreover, it can be seen from Fig. 2f that CuSCN, having an intrinsic trigonal pyramid shape [15], covered the top of ZnO

rod arrays only when the gaps of the arrays had been totally filled. Fig. 2g and h is the samples deposited at 20 °C, it can be found that the CuSCN deposition at 0 °C was more compactly filled with smaller CuSCN grains, comparing with those deposited at 20 °C. However, from the above FESEM observation, the CuSCN growth behavior still maintained its intrinsic

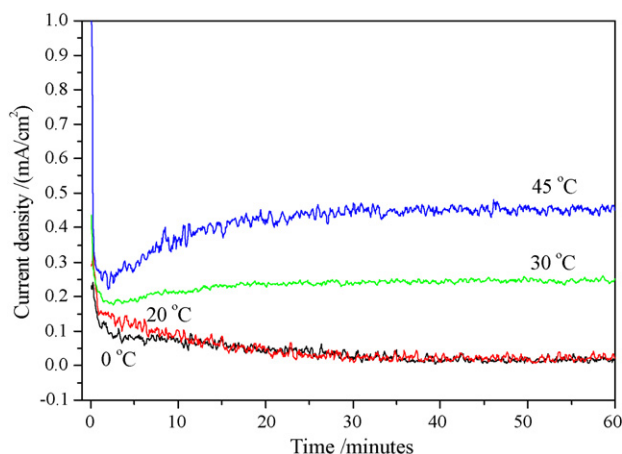


Fig. 3. Current density as a function of time for potentiostatic deposition of -500 mV on the ZnO rod arrays substrates at different deposition temperatures.

trigonal pyramid shape, which would deteriorate the compact filling of CuSCN in the gaps of ZnO rod arrays, especially at a high temperature. So, the present electrodeposition system of CuSCN should be improved by the optimization of the electrolyte solution to improve the interface chemical behavior so as to get finer grains and restrain the free growth of trigonal pyramid grains, and finally achieving the total filling of ZnO rod arrays.

Fig. 3 shows the curves of current density as a function of time for potentiostatic deposition of -500 mV on the ZnO rod arrays substrates at different deposition temperatures. As the chronoamperometry measurements are shown in Fig. 3, the current densities rapidly decreased at the onset of the applied cathodic potentials on the four curves, which may be attributed to the induction process (the charge–discharge process of double layer) at the interface of electrode/electrolyte solution. It should be noted that the initial value of current density beyond the induction process was rather different at different temperatures, and it changed from about 0.11 – 0.27 mA/cm² with the increasing of temperature from 0 °C to 45 °C, indicating a strong temperature dependence. Compared between depositions at temperatures 0 °C and 20 °C, the current density of the sample deposited at 20 °C was higher than that of the sample deposited at 0 °C, especially in the early 10 min. Moreover, both current densities became rather low beyond 40 min, indicating a low rate and steady state growth of CuSCN. For deposition at higher temperatures, such as 30 °C and 45 °C, the change of current density depending on temperature is more remarkable. Obviously, high current densities tended to result in high growth rate of CuSCN with large grain size [15]. On the other hand, the samples deposited at 45 °C apparently presented brown-colored points dispersed on the film surface, indicating the Cu co-deposition [15].

Fig. 4 shows the electrochemical behaviors in the deposition systems at the temperature of 0 °C. Curve II is linear sweep voltammetric (LSV) characteristic of ZnO rod arrays and curve I is performed on a bare ITO substrate, shown as reference. We can see that the cathodic threshold potential for deposition of CuSCN on ZnO rod arrays is about -180 mV. Subsequent

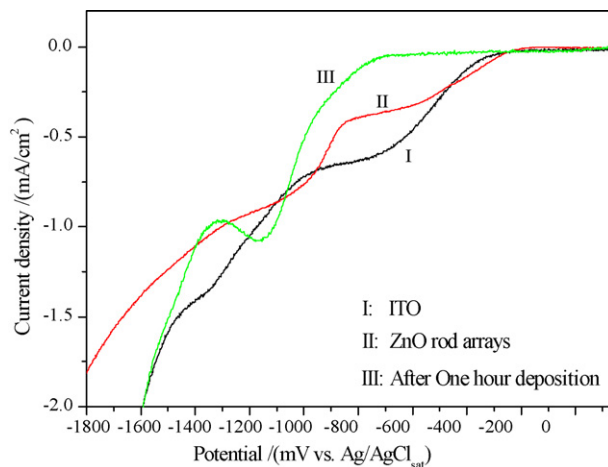


Fig. 4. Linear sweep voltammetric curves on (I) bare ITO, (II) ZnO rod arrays and (III) CuSCN-coated ZnO rod arrays substrate after 1 h deposition at 0 °C. The scan rate is 50 mV s⁻¹.

increase of cathodic current densities is in the potential range of -180 mV to -700 mV, indicating that the reduction reaction of $\text{Cu}^{2+} + e^- \rightarrow \text{Cu}^+$ occurred, which is a crucial step for CuSCN deposition. Compared with curve II on ZnO rod arrays, the cathodic threshold potential on ITO substrate is more negative and about -220 mV. The slight shift of the cathodic threshold of ZnO rod arrays toward a little more positive potential may be attributed to the surface states existing on ZnO rods. It is known that the as-grown ZnO is an n-type semiconductor with intrinsic defects, such as oxygen vacancies and Zn interstitials [17]. These defects will be easy to form some surface states on ZnO rods. In addition, when a semiconductor electrode is placed in an electrolyte solution, adsorption of the ions in the electrolyte also contributes to the formation of surface states [18]. The surface states noticeably improve the transfer of the electrons on the interface of the semiconductor electrode/electrolyte solution during the deposition reaction, causing the earlier cathodic reduction current. Furthermore, it can be seen from Fig. 4 that the cathodic current density on ZnO rod arrays in the range of -200 mV to -450 mV is slightly higher than that of the ITO substrate, which is caused by the earlier threshold potential of the reduction reaction on ZnO rod arrays. After the potential of -450 mV, the cathodic current density becomes smaller, which is likely due to the space barrier in interface region consisting of ZnO rod arrays and liquid electrolyte, leading to a potential drop.

Fig. 4 also shows the LSV curve on the CuSCN-coated ZnO rod arrays following a 1 h deposition (curve III). It can be determined that there is not a cathodic reduction reaction current until -700 mV, showing a negative shift of -520 mV compared with that on the bare ZnO rod arrays. In this circumstance, the electrons transfer from the conduction band of the deposited CuSCN layer to the reaction interface or the holes transfer from the reaction interface to the valence band of CuSCN as the reduction of $\text{Cu}^{2+} + e^- \rightarrow \text{Cu}^+$ has been restricted in the potential range of -180 mV to -700 mV. Actually, the appreciated potential range of sole CuSCN deposition is in the range from -180 mV to -500 mV. While over -500 mV, Cu co-deposition

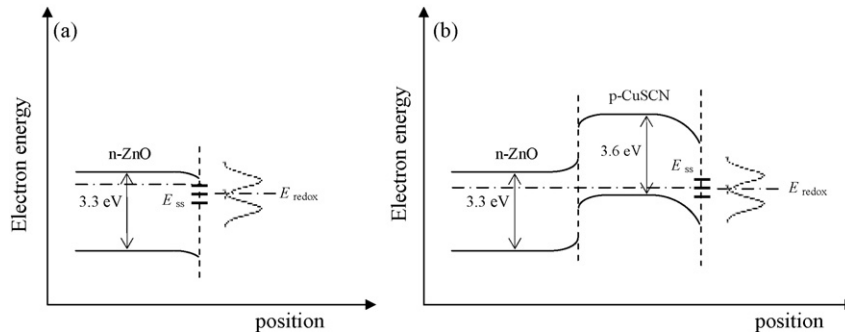


Fig. 5. Schematic of the energy band model of (a) the initial deposition on ZnO rod arrays and (b) ZnO/CuSCN heterojunction/electrolyte solution at negative external potential.

will occur [15]. It implied that the increase of current density over -700 mV on curve III is caused by the deposition of metal Cu. Thus, according to the above LSV measurements, we proposed an energy band model for the electrodeposition of CuSCN on ZnO rod arrays. Fig. 5a is the energy band model concerning the initial deposition on the bare ZnO rod arrays under a negative external potential. In the initial stage, the growth of CuSCN was a conduction process, in which the electrons could easily transfer from ZnO rods to electrolyte solution. Once the CuSCN layer covered the surface of ZnO rods, the carrier transfer mechanism was invalid. The successive deposition of CuSCN should be based on the energy band model concerning the ZnO/CuSCN junction/electrolyte solution at the negative applied potential, as shown in Fig. 5b. The energy band contact at the reaction interface converted from n-ZnO/electrolyte to p-CuSCN/electrolyte. As mentioned above, the carrier transfer through the formed CuSCN layer for successive growth of CuSCN was restricted. Thus, the following deposition mechanism could be explained according to the thermal activation of surface states. Wu et al. [13] has suggested a thermal activation mechanism of surface states to describe the electrodeposition of CuSCN on conducting ITO substrate. In fact, the adsorption of SCN^- anions and Cu^{2+} cations at the electrode interface, especially the adsorption of Cu^{2+} cations due to the applied negative potential, served as a key role in building of the surface states [18], as well as the temperature-dependent electron state of the surface state also played another important role. Both affected by temperature dominated the successive electrodeposition process on the CuSCN-coated ZnO rod arrays. In terms of this deposition mechanism, it could conclude that the original nucleation and grain growth of CuSCN occurred on bare ZnO rods during the conduction band process were prior. The following growth of CuSCN was slow and based on the thermal activation of surface states controlled by temperature. Fig. 2a–f confirmed the above growth mechanism that the growth of CuSCN was prior to filling of the gaps of the ZnO rod arrays. And the significant increases of current density with deposition temperatures, as shown in Fig. 3, also demonstrated the function of thermal activation governed by temperature. So, according to the thermal activation growth mechanism, a high deposition temperature could lead to a faster growth rate of CuSCN on ZnO rod arrays. Nevertheless, the intrinsic growth of trigonal pyramid grains and Cu co-deposition at higher temperature must be avoided

in order to achieve the total filling and promise the quality of the junction. On the other hand, the diffusion of Cu^{2+} ions in the form of the Cu(II)–TEA complexes at different temperatures will also impact the deposition, which needs specific investigation in further.

Fig. 6 shows the electrical measurements of the prepared CuSCN/ZnO rod array interpenetrating junctions. I – V characteristics of the p-CuSCN/n-ZnO rod arrays heterojunctions formed within 1 h of deposition under 0°C and 20°C are shown in Fig. 6a. The inset exhibited linear I – V characteristic of the contact between ITO and p-CuSCN film, indicating an ohmic contact formed between ITO and electrodeposited CuSCN film. So the rectification in Fig. 6a was naturally attributed to the junction properties of the electrodeposited CuSCN/ZnO rod array interpenetrating heterojunctions. In Fig. 6a, the two I – V curves clearly exhibit the almost exponential increase of current density under forward bias. For the heterojunction deposited at 20°C , the turn-on voltage is approximately 0 V and the reverse current does not saturate in the reverse bias range. The rectification ratio, measured at the applied voltage of ± 0.5 V, is only about 6, implying a weak-rectifying effect. For the heterojunction deposited at 0°C , the turn-on voltage is about 0.3 V. The reverse bias current density saturates in a reverse bias range of 0 V to -0.5 V and is about 5×10^{-3} mA/cm². The rectification ratio, also measured at ± 0.5 V, is about 19. The larger rectification ratio of the heterojunction formed at 0°C , compared with the one deposited at 20°C , indicates that the heterojunction deposited at low temperature has a better electrical contact.

Fig. 6b shows the semilog plot of current density versus forward bias voltage of the two heterojunctions. Based on Fig. 3b, the diode ideality factor and series resistance were evaluated according to the empirical equation [19]:

$$I = I_0 \left[\exp \left(q \left(\frac{V - IR_S}{nkT} \right) - 1 \right) \right] \quad (1)$$

where I_0 is the reverse bias saturation current, and k , T , n and R_S are Boltzmann's constant, temperature, diode ideality factor and series resistance, respectively. For the heterojunction deposited at 20°C , in the low forward bias voltage range, it seems that there is not a straight line region, making it difficult to estimate the diode ideality factor. Nevertheless, we still estimated the series resistance of this junction to be about 240Ω . However,

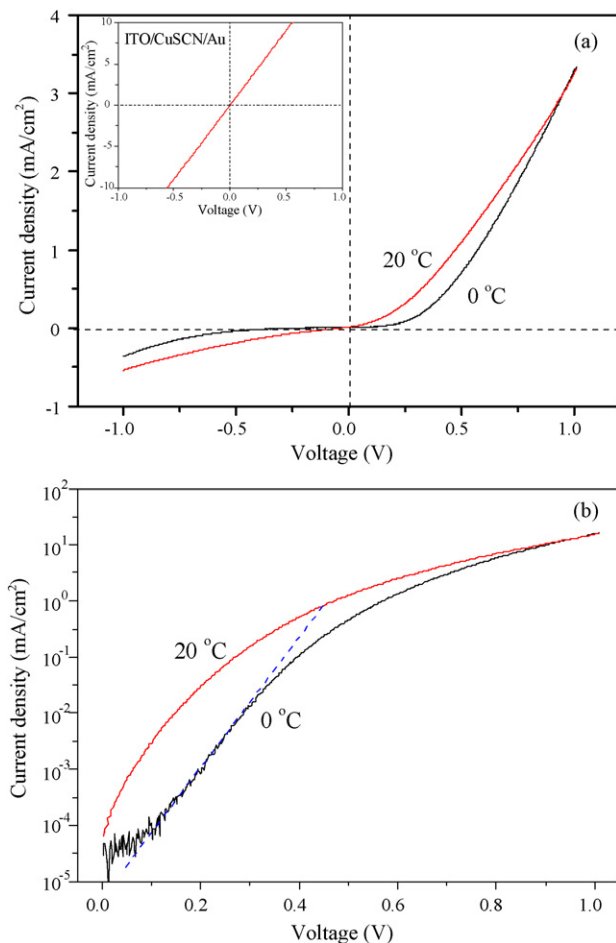


Fig. 6. (a) I - V characteristics of CuSCN/ZnO rod arrays p-n heterojunctions prepared in weak basic electrolyte solution at deposition temperature of 0 °C and 20 °C under -500 mV, and (b) Semilog plot of current density versus forward bias voltage of the p-n heterojunctions. The inset in (a) is I - V characteristics of ohmic contact between ITO/CuSCN/Au junction and ITO/Au junction, shown as a reference in which the CuSCN film was prepared in the same weak basic electrolyte solution at deposition temperature of 20 °C under -500 mV after 1 h.

for the heterojunction formed at 0 °C, the diode ideality factor is about 3.3 in the low forward bias voltage range of 0.15–0.4 V, and the series resistance is about 130 Ω . Thus, these result suggest that the electrical contact of the heterojunction formed at 0 °C is better than that of the one formed at 20 °C. The better heterojunction properties imply that the CuSCN has been better filled in the ZnO rods, and the contact between electrodeposited CuSCN and ZnO rods was compact, which was also confirmed by the FESEM observation. In addition, according to the Sah–Noyce–Shockley theory [20], in a p-n junction, the value of the ideality factor is 1.0 at a low voltage, and 2.0 at a higher voltage. The ideality factor of the rod-type heterojunction is quite large, which may be due to: (1) the total filling among the ZnO rod arrays did not achieve completely; (2) the large series resistance of ZnO rod arrays embedded heterostructures [21]; (3) the existence of the surface states, which could also lead to a large diode ideality [22]. So in order to improve the electrical properties of the interpenetrating heterojunctions, the total filling of the ZnO rod arrays should be firstly promised. The aspect

ratio of the rod arrays as well as the surface modification also needs to be tailored carefully.

4. Conclusions

p-CuSCN/n-ZnO rod array heterostructures were successfully electrodeposited by using a weakly basic electrolyte solution to avoid the acidic etching of the ZnO substrates. From the FESEM observation, CuSCN was able to sufficiently embed in the gaps of the ZnO rod arrays, and grow thicker to cover the ZnO rod arrays substrate. The chronoamperometry measurements revealed that a high deposition temperature led to a higher current density, implying faster growth of CuSCN on ZnO rod arrays with larger grain size. However, the high temperature also resulted in the emergence of Cu co-deposition. According to the LSV analysis, the energy band models for the electrodeposition of CuSCN on ZnO rod arrays suggested that the initial growth of CuSCN on bare ZnO substrate was a conduction band process, which caused the prior filling in the gaps of ZnO rod arrays. Successive growth of CuSCN on the formed ZnO/CuSCN heterojunction was dominated by the thermal activation mechanism of surface states, which could be directly controlled by the deposition temperature. The p-CuSCN/n-ZnO interpenetrating heterojunctions deposited at both 0 °C and 20 °C showed clear rectification and the heterojunction formed at 0 °C exhibited better diode properties. Lower deposition temperature is preferred to better electrical contact of the heterojunction so far as the thermal activation mechanism at such low temperature is available. The further study should be focused on the optimization of the electrodeposition solution system and the deposition parameters so as to obtain high quality heterojunctions.

Acknowledgement

The authors wish to acknowledge the financial support of Key Basic Research of TSTC (Project No. 07JCZDJC009900).

References

- [1] B. O'Regan, D.T. Schwartz, S.M. Zakeeruddin, M. Grätzel, *Adv. Mater.* 12 (2000) 1263.
- [2] C.L. Clément, R.T. Zaera, M.A. Ryan, A. Katty, G. Hodes, *Adv. Mater.* 17 (2005) 1512.
- [3] B. O'Regan, M. Grätzel, *Nature* 353 (1991) 737.
- [4] K. Tennakone, G.R.R.A. Kumara, I.R.M. Kottegoda, V.P.S. Perera, P.S.R.S. Weerasundara, *J. Photochem. Photobiol. A: Chem.* 117 (1998) 137.
- [5] M. Law, L. Greene, J.C. Johnson, R. Saykally, P.D. Yang, *Nat. Mater.* 4 (2005) 455.
- [6] B. O'Regan, D.T. Schwartz, *Chem. Mater.* 7 (1995) 1349.
- [7] B. Li, L. Wang, B. Kang, P. Wang, Y. Qiu, *Sol. Energy Mater. Sol. Cells* 90 (2006) 549.
- [8] G.R.R.A. Kumara, A. Konno, G.K.R. Senadeera, P.V.V. Jayaweera, D.B.R.A. De Silva, K. Tennakone, *Sol. Energy Mater. Sol. Cells* 69 (2001) 195.
- [9] B.R. Sankapal, E. Goncalves, A. Ennaoui, M.C. Lux-Steiner, *Thin Solid Films* 451/452 (2004) 128.
- [10] K. Tennakone, A.R. Kumarasinghe, P.M. Sirmanne, G.R.R.A. Kumara, *Thin Solid Films* 261 (1995) 307.

- [11] C. Rost, I. Sieber, S. Siebentritt, M.C. Lux-Steiner, R. Konenkamp, *Appl. Phys. Lett.* 75 (1999) 692.
- [12] B. O'Regan, D.T. Schwartz, *J. Appl. Phys.* 80 (1996) 4749.
- [13] W. Wu, Z. Jin, Z. Hua, Y. Fu, J. Qiu, *Electrochim. Acta* 50 (2005) 2343.
- [14] W. Wu, Z. Jin, G. Hu, S. Bu, *Electrochem. Acta* 52 (2007) 4804.
- [15] Y. Ni, Z. Jin, Y. Fu, *J. Am. Ceram. Soc.* 90 (2007) 2966.
- [16] K. Yu, Z. Jin, X. Liu, J. Zhao, J. Feng, *Appl. Surf. Sci.* 253 (2007) 4072.
- [17] Ü. Özgür, Y.I. Alivov, C. Liu, A. Teke, M.A. Reshchikov, S. Dogan, V. Avrutin, S.J. Cho, H. Morkoç, *J. Appl. Phys.* 98 (2005) 041301.
- [18] S.R. Morrison, *Electrochemistry at Semiconductor and Oxidized Metal Electrodes*, Plenum, New York, 1980.
- [19] R.F. Pierret, *Semiconductor Device Fundamentals*, Addison-Wesley, New York, 1996.
- [20] C.T. Sah, R.N. Noyce, W. Shockley, *Proc. IRE* 45 (1957) 1228.
- [21] M.C. Jeong, B.Y. Oh, M.H. Ham, J.M. Myoung, *Appl. Phys. Lett.* 88 (2006) 202105.
- [22] H.P. Maruska, F. Namavar, N.M. Kalkhoran, *Appl. Phys. Lett.* 61 (1992) 1338.